The Astrophysical Journal Letters, 817:L5 (6pp), 2016 January 20 doi:10.3847/2041-8205/817/1/L5

NEW ASTROPHYSICAL REACTION RATE FOR THE $^{12}C(\alpha, \gamma)^{16}O$ REACTION

Zhen-Dong An[1,2], Yu-Gang Ma[1,3], Gong-Tao Fan[1], Yong-Jiang Li[1], Zhen-Peng Chen[4], and Ye-Ying Sun[5]
[1] Shanghai Institute of Applied Physics, Chinese Academy of Sciences, Shanghai 201800, China; ygma@sinap.ac.cn
[2] University of Chinese Academy of Sciences, Beijing 100049, China
[3] ShanghaiTech University, Shanghai 200031, China
[4] Department of Physics, Tsinghua University, Beijing 100084, China; zhpchen@tsinghua.edu.cn
[5] Department of Materials, Tsinghua University, Beijing 100084, China
Received 2015 October 20; accepted 2015 December 30; published 2016 January 19

ABSTRACT

A new astrophysical reaction rate for $^{12}C(\alpha, \gamma)^{16}O$ has been evaluated on the basis of a global *R*-matrix fitting to the available experimental data. The reaction rates of $^{12}C(\alpha, \gamma)^{16}O$ for stellar temperatures between $0.04 \leqslant T_9 \leqslant 10$ are provided in a tabular form and by an analytical fitting expression. At $T_9 = 0.2$, the reaction rate is $(7.83 \pm 0.35) \times 10^{15}\,\mathrm{cm^3\,mol^{-1}\,s^{-1}}$, where stellar helium burning occurs.

Key words: Galaxy: abundances – nuclear reactions, nucleosynthesis, abundances – stars: abundances – stars: evolution – supernovae: general

1. INTRODUCTION

Astrophysical reaction rates are of great importance in studies of the stellar nucleosynthesis and the stellar evolution. During stellar helium burning, the rates of 3α and the $^{12}C(\alpha, \gamma)^{16}O$ reaction, in competition with one another, determine the timescale of this phase and the relative abundances of ^{12}C and ^{16}O in a massive star. The reaction rate of the 3α process is known to have an uncertainty of about 10% (Fynbo et al. 2005), at astrophysical temperatures (0.2×10^9 K); while such accuracy is not the case for the $^{12}C(\alpha, \gamma)^{16}O$ reaction, yet relevant for the rise time of the SN I light curves (Dominguez et al. 2001), the production of important radioactive nuclei ^{26}Al, ^{44}Ti, and ^{60}Fe (Tur et al. 2010), the size and mass of Fe core for a pre-supernova star (Woosley et al. 2003), and the formation of X-ray black hole binaries (Brown et al. 2001) and neutron stars (Brown & Bildsten 1998; Wen & Zhou 2013) in massive stars.

Experimental investigations of the reaction rate $N_A \langle \sigma v \rangle$ are calculated with the following standard formula (Rolfs & Rodney 1988),

$$N_A \langle \sigma v \rangle = \left(\frac{8}{\pi\mu}\right)^{1/2} \frac{N_A}{(k_B T)^{3/2}} \times \int_0^\infty dE S(E) \exp\left(-\sqrt{\frac{E_G}{E}} - \frac{E}{k_B T}\right), \quad (1)$$

where N_A refers to the Avogadro's constant, μ is the reduced mass of the entrance channel, $^{12}C+\alpha$, k_B is the Boltzmann constant, and $E_G = (2\pi\alpha Z_\alpha Z_C)^2 \mu c^2/2$ is the Gamow energy with the fine-structure constant α. The function $S(E) = \sigma(E) E \exp(2\pi\eta)$ is the total S factor of $^{12}C(\alpha, \gamma)^{16}O$, where $\eta = Z_\alpha Z_C e^2/(\hbar v)$ is the Sommerfeld parameter and $\sigma(E)$ is the cross section. For each temperature of T_9 (temperature in units of 10^9 K), the rate is obtained by Equation (1) with corresponding data for the $S(E)$ factor.

The difficulty in measuring the S factor of the $^{12}C(\alpha, \gamma)^{16}O$ reaction results from the extremely small $\sigma(E_0)$, which is about 10^{-17} b at 0.3 MeV, where the helium burning occurs. The observed $S(E)$ factors are focused on the energy region of $E_{c.m.} > 0.9$ MeV, which means that an extrapolation cannot currently be evaded. It remains a challenging task to obtain the $S(E)$ factor for the $^{12}C(\alpha, \gamma)^{16}O$ reaction in part due to the complicated level structure of the ^{16}O nucleus (deBoer et al. 2013; Ma et al. 2014).

The $^{12}C(\alpha, \gamma)^{16}O$ reaction rates at astrophysical temperatures are dominated by resonances states in the compound nucleus ^{16}O. The rates based upon the different extrapolation and fitting models to the parts of existing $S(E)$ factor measurements, such as potential models and the *R*-matrix (or *K*-matrix) theory, were reported by several research teams. Representative results for the rates from the *R*-matrix (or *K*-matrix) theory were provided by Caughlan & Fowler (1988; hereafter CF88), Buchmann (1996), Angulo et al. (1999; hereafter NACRE), and Kunz et al. (2002). Two recent compilations, Katsuma (2012) and Xu et al. (2013; hereafter NACRE II), are mainly based on the potential models. However, for the corresponding reaction rate of these compilations, at $T_9 = 0.2$, the published S-factor at 0.3 MeV disagrees at the 10% level (see Table 1 of An et al. 2015) with the quoted uncertainties that are about twice as large as estimated for precision modeling efforts (Woosley & Heger 2007).

In An et al. (2015), we report a reduced *R*-matrix theory to make the global fitting to plenty of complementary experimental data about the ^{16}O compound nucleus. These complementary data effectively help us to understand the concrete effect of the ^{16}O nucleus for the $S(E)$ factor and the reaction rate. Based on the published S factor estimates, the updated astrophysical reaction rates of $^{12}C(\alpha, \gamma)^{16}O$ are presented and compared with the previously published reaction rates in this paper.

2. REACTION RATES

2.1. The Uncertainty of S-factors

The S-factors of $^{12}C(\alpha, \gamma)^{16}O$ are constituted by several resonant peaks with strong interference patterns. Furthermore, the complicated mechanism of this reaction results in unpredictable interference effects from the first principles (Kunz et al. 2002). The global fitting for the ^{16}O system with a multilevel, multichannel *R*-matrix allows for the simultaneous analysis of differential cross-section data and an the corresponding angle-integrated cross section of an ^{16}O compound

Table 1
The $^{12}C(\alpha, \gamma)^{16}O$ Reaction Rates (in $cm^3\ mol^{-1}\ s^{-1}$)

T_9	$N_A\langle\sigma v\rangle$	High	Low	10^n	T_9	$N_A\langle\sigma v\rangle$	High	Low	10^n
0.040	9.27	9.75	8.79	−31	0.60	3.28	3.40	3.17	−8
0.042	3.94	4.14	3.74	−30	0.65	8.00	8.27	7.73	−8
0.045	2.92	3.07	2.77	−29	0.70	1.78	1.84	1.73	−7
0.050	5.69	5.98	5.40	−28	0.75	3.70	3.82	3.58	−7
0.055	7.60	7.98	7.21	−27	0.80	7.19	7.42	6.96	−7
0.060	7.51	7.88	7.13	−26	0.85	1.32	1.37	1.28	−6
0.065	5.81	6.10	5.52	−25	0.90	2.33	2.40	2.26	−6
0.070	3.67	3.85	3.49	−24	0.95	3.93	4.05	3.81	−6
0.075	1.95	2.05	1.86	−23	1.00	6.41	6.60	6.22	−6
0.080	9.00	9.44	8.57	−23	1.10	1.56	1.60	1.51	−5
0.085	3.66	3.84	3.49	−22	1.20	3.42	3.52	3.33	−5
0.090	1.34	1.40	1.27	−21	1.30	6.96	7.15	6.78	−5
0.095	4.45	4.67	4.24	−21	1.40	1.33	1.36	1.30	−4
0.100	1.36	1.43	1.30	−20	1.50	2.41	2.47	2.35	−4
0.105	3.88	4.06	3.69	−20	1.60	4.19	4.29	4.09	−4
0.11	1.03	1.08	0.98	−19	1.70	7.02	7.18	6.85	−4
0.12	6.18	6.48	5.89	−19	1.80	1.14	1.16	1.11	−3
0.13	3.06	3.20	2.91	−18	1.90	1.80	1.83	1.76	−3
0.14	1.29	1.35	1.23	−17	2.00	2.76	2.82	2.71	−3
0.15	4.75	4.97	4.53	−17	2.10	4.15	4.23	4.07	−3
0.16	1.56	1.64	1.49	−16	2.20	6.10	6.22	5.98	−3
0.17	4.67	4.88	4.46	−16	2.30	8.79	8.96	8.62	−3
0.18	1.28	1.34	1.23	−15	2.50	1.73	1.76	1.69	−2
0.19	3.27	3.42	3.13	−15	2.75	3.66	3.73	3.60	−2
0.20	7.83	8.18	7.48	−15	3.00	7.13	7.26	7.00	−2
0.21	1.77	1.85	1.69	−14	3.25	1.29	1.32	1.27	−1
0.22	3.79	3.96	3.63	−14	3.50	2.20	2.24	2.16	−1
0.24	1.53	1.59	1.46	−13	3.75	3.58	3.64	3.51	−1
0.26	5.29	5.52	5.07	−13	4.00	5.57	5.67	5.46	−1
0.28	1.62	1.69	1.55	−12	4.25	8.37	8.54	8.21	−1
0.30	4.47	4.66	4.29	−12	4.50	1.22	1.25	1.20	0
0.32	1.13	1.18	1.08	−11	5.00	2.42	2.48	2.36	0
0.34	2.65	2.75	2.54	−11	5.50	4.43	4.56	4.31	0
0.36	5.81	6.04	5.57	−11	6.00	7.60	7.87	7.34	0
0.38	1.20	1.25	1.15	−10	6.50	1.23	1.28	1.18	1
0.40	2.37	2.46	2.27	−10	7.00	1.90	1.99	1.81	1
0.42	4.46	4.63	4.28	−10	7.50	2.79	2.94	2.64	1
0.45	1.07	1.11	1.03	−9	8.00	3.95	4.18	3.71	1
0.50	3.91	4.05	3.76	−9	9.00	7.13	7.63	6.64	1
0.55	1.21	1.25	1.17	−8	10.0	1.15	1.24	1.06	2

nucleus (An et al. 2015). A multichannel *R*-matrix analysis provides the possibility of reducing uncertainties in the extrapolated total and partial S-factors of the $^{12}C(\alpha, \gamma)^{16}O$ reaction, and the interpretation of the interference mechanism via the additional constraint offered by the simultaneous analysis of multiple reaction channels (Azuma et al. 2010).

The error propagation formulae (Smith 1991) are adopted to determine the uncertainty of the *S* factor in the whole energy region. Our extrapolation value is $S_{tot}(0.3\ MeV) = 162.7 \pm 7.3\ keV$ b, which is composed of $S_{E10}(0.3\ MeV) = 98.0 \pm 7.0\ keV$ b, $S_{E20}(0.3\ MeV) = 56.0 \pm 4.1\ keV$ b ground-state captures and of cascade captures, $S_{casc}(0.3\ MeV) = 8.7 \pm 1.8\ keV$ b. Furthermore, the cascade transitions of $S_{6.05}$ and $S_{6.13}$ at 0.3 MeV are 4.91 ± 1.11 keV.b and 0.16 ± 0.26 keV b, respectively. They are quite consistent with the constructive interference result of $S_{6.05}$ (0.3 MeV) $= 4.36 \pm 0.45$ keV.b and destructive interference of $S_{6.13}$ (0.3 MeV) $= 0.12 \pm 0.04$ keV b of Avila et al. (2015), which constrained the contribution of the values by measuring the asymptotic normalization coefficients (ANCs) for these states using the α-transfer reaction $^6Li(^{12}C, d)^{16}O$. We adopt a similar approach for the fitting of cascade transitions. This is one of the reasons that uncertainty of the extrapolated *S* factor reduces dramatically. The values of the other two cascade transitions are $S_{7.12}$ (0.3 MeV) $= 0.63 \pm 0.22$ keV b and $S_{6.92}(0.3\ MeV) = 3.00 \pm 0.42$ keV b, which are in excellent agreement with the recent results of Schürmann et al. (2012), respectively.

2.2. New Reaction Rate for $^{12}C(\alpha, \gamma)^{16}O$

The absolute values of reaction rates, $N_A\langle\sigma v\rangle$ of $^{12}C(\alpha, \gamma)^{16}O$ can be obtained by Equation (1) from the self-consistent total *S* factor and its uncertainties. Table 1 lists 80 points of reaction rates in the temperature range of $0.04 \leqslant T_9 \leqslant 10$. To be precise, the total reaction rate of $^{12}C(\alpha, \gamma)^{16}O$ is achieved after multiplying $N_A\langle\sigma v\rangle$ with the probability densities of the reaction partners and integrating over the energy interval. The uncertainties of the reaction rates obtained from our *R*-matrix model are also tabulated for the high rate and the low rate in Table 1.

According to the Gamow theory (Rolfs & Rodney 1988), for the nonresonant cross section, the Gamow window (significant

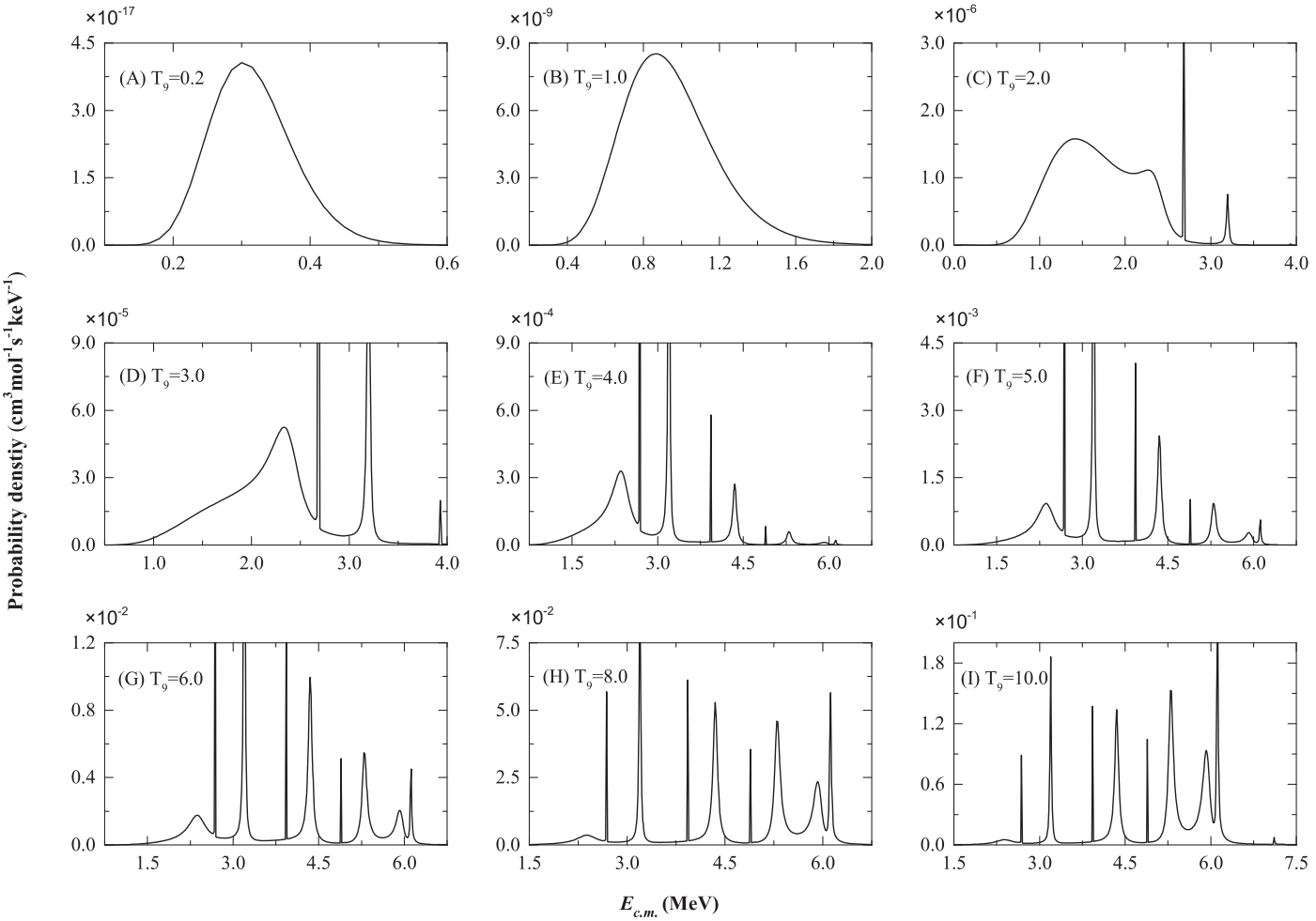

Figure 1. Reaction rate probability density functions for $^{12}C(\alpha, \gamma)^{16}O$ at different values of T_9.

integral interval) of each T_9 is selected in $[E_0 - \Delta E_0/2, E_0 + \Delta E_0/2]$, with $E_0 = (E_G^{1/2} k_B T/2)^{2/3}$ and $\Delta E_0 = (16 E_0 k_B T/3)^{1/2}$. Considering the typical T_9 temperatures involved, we have $E_0 = 0.3$ MeV of helium burning starting at $T_9 = 0.2$. Furthermore, for the S factor data, the chief center-of-mass energy range is 0.1–0.5 MeV. As E_0 and ΔE_0 increase with stellar temperature, the $S(E)$ factor data in the higher energy range gradually play a leading role for the reaction rate.

To understand the influence of the $S(E)$ factor of $^{12}C(\alpha, \gamma)^{16}O$ on the reaction rate at different temperatures, probability density functions of the total reaction rates at $T_9 = 0.2$, 1.0, 2.0, 3.0, 4.0, 5.0, 6.0, 8.0, and 10.0 are shown in Figure 1. At $T_9 = 0.2$ and 1.0, the probability density functions are located almost in the extrapolated S factor, without resonance peaks, so the Gamow window can be well approximated by a Gaussian distribution with the most effective energy $E_0 = 0.3$ MeV and $E_0 = 0.9$ MeV. As the T_9 increases from 1 to 10, however, the influence of resonances of the $S(E)$ factor becomes more and more remarkable, and the probability density functions can no longer be approximated by the Gaussian distribution. So, the $^{12}C(\alpha, \gamma)^{16}O$ reaction rate at these temperatures can be obtained just by the S factor measurements at energies as wide as possible.

The S_{tot} measurements of Schürmann et al. (2005, 2011), in reverse kinematics using the recoil mass separator, allowed us to acquire data with a high degree of accuracy (<3%) in a wide energy scope of $E_{c.m.} = 1.5$–4.9 MeV. These data would provide good restrictions on the probability density functions of $T_9 = 2.0$, 3.0, and 4.0 (Figures 1(C)–(E)), and the uncertainties of the $^{12}C(\alpha, \gamma)^{16}O$ reaction rate are smaller than 3%, from $2.0 \leqslant T_9 \leqslant 4.0$.

Kunz et al. (2002) studied the S factor in the ground state of $^{12}C(\alpha, \gamma)^{16}O$ at higher energies, covering the 1_3^- ($E_{c.m.} = 5.28$ MeV) and 1_4^- ($E_{c.m.} = 5.93$ MeV), using resonance parameters of Tilley et al. (1993) in the calculation. The published data in two independent experiments (Brochard et al. 1973; Ophel et al. 1976) of the ground-state transition were neglected. Possible interference effects were included in the calculation of S_{E10} and S_{E20} by applying the R-matrix fitting procedures, but they were somewhat speculative, and the results of $S_{g.s}$ were about $2 \sim 5$ times away from experimental data. Therefore, from the probability density functions of $T_9 = 5.0$, 6.0, 8.0, and 10.0 (Figures 1(F)–(I)), it can be inferred that the rate calculation of Kunz et al. (2002) is significantly higher.

The S_{tot} can be indicated according to different types of J^π (0^+, 1^-, 2^+, 3^-, and 4^+). Figure 2(A) shows the fractional contributions of different values of J^π compared to the total reaction rates in $0.04 \leqslant T_9 \leqslant 10.0$. It can be seen that $J^\pi = 1^-$ and 2^+ dominate the reaction rate up to $T_9 = 2.0$. From the probability density functions of $T_9 = 0.2$, 1.0, and 2.0 (Figures 1(A)–(C)), we note that the contribution stems mainly from $J^\pi = 1^-$ ($E_{c.m.} = 2.42$ MeV) and $J^\pi = 2^+$ ($E_{c.m.} =$

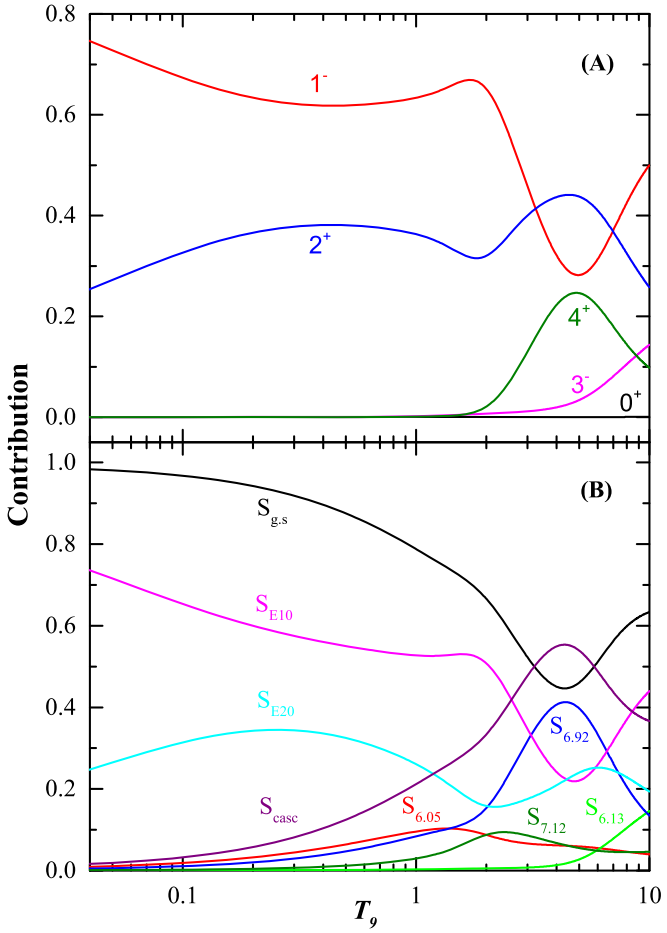

Figure 2. Top: fractional contributions of different J^{π} to the total reaction rates of $^{12}C(\alpha, \gamma)^{16}O$. Bottom: fractional contributions of $S_{g.s.}$ (including E_{10} and E_{20} to the ground state) and the cascade transitions to the total rates.

2.58 MeV) levels in ^{16}O. The rate above $T_9 = 2.0$, the fraction from 3^- gradually increases with temperature. This comes from the contribution of $J^{\pi} = 3^-$ ($E_{c.m.} = 4.44$, 5.97, and 6.10 MeV) resonances. The contribution of $J^{\pi} = 4^+$ increases with T_9 first, and then decreases, having two 4^+ resonances just at $E_{c.m.} = 3.20$ and 3.93 MeV in the integral interval. Thus, the fractional contributions of different values of J^{π} reconfirmed the validity of the probability density functions in Figure 1.

The contributions of ground-state capture and cascade captures to the reaction rate of $^{12}C(\alpha, \gamma)^{16}O$ are illustrated in Figure 2(B). Ground state capture (S_{E10} and S_{E20}) dominates the reaction rate up to $T_9 = 0.1$. Furthermore, the contributions from the cascade transitions increase with T_9. Besides at the important He-burning temperature $T_9 = 0.2$, the rate is still important all the way up to $T_9 = 5.0$, because the inverse reaction of $^{12}C(\alpha, \gamma)^{16}O$ plays an important role in silicon burning (S. E. Woosley 2013, private communication). Thus, the cascade transition is necessary for the precise calculation of the reaction rate.

2.3. Comparison to Other $^{12}C(\alpha, \gamma)^{16}O$ Determinations

Figure 3 shows comparisons between our new reaction rate and previous estimates. In each panel, the dashed line shows the ratio of a previous determination to our new rate. The gray bands are the uncertainty of the published rate, e.g., in Figure 3 (A), the edges of the gray zone are reaction rate ratios of NARCE II's limits to the principal value of our rates. The blue bands estimate the uncertainty of our rate. Below $T_9 \approx 4.0$, our recommended results are within the uncertainties of Buchmann (1996), Kunz et al. (2002), and NACRE II. Above $T_9 = 4$, the results agree with the analysis of NACRE.

By comparing all of the published rates with our present results, the principal values of each rate are shown in Figure 4. At an astrophysical temperature of $T_9 = 0.2$, the new rate is about 10% larger than the rate of NACRE II (S_{tot} (0.3 MeV) = 148 ± 27 keV b) and Buchmann (1996) (S_{tot} (0.3 MeV) = 146 keV b), about 16% lower than the rate of the NACRE (S_{tot}(0.3 MeV) = 199 ± 64 keV b), and it is quite consistent with the adopted value of Kunz et al. (2002) (S_{tot} (0.3 MeV) = 165 ± 50 keV b).

In the intermediate range of $0.5 \leqslant T_9 \leqslant 3$, our recommended rate is in good agreement with NACRE II. The temperature dependence of our recommended value differs significantly from the rates of Katsuma (2012), which stems from the higher total S factor at 1_2^- ($E_{c.m.} = 2.42$ MeV) resonance-peak, overestimating the cross section of Schürmann et al. (2005) in their calculations (Katsuma 2008). In the same temperature range, the deviation from Kunz et al. (2002) mainly originates from the lower calculation values of the total S factor from $E_{c.m.} = 0.5$ MeV to $E_{c.m.} = 2.0$ MeV. The lower value of NACRE is a direct consequence of the considered cascade transitions for the total S-factors.

For the rates above $T_9 = 3$, our reaction rate increases with T_9, but has lower values than Kunz et al. (2002) and NACRE II, because the high-energy data covering the 1_3^- and 1_4^- resonance are apparently overestimated in their calculations.

2.4. Analytical Formula

A common form of reaction rate is an analytical formula with an appropriate parametrization for applications in stellar models. Equation (2) is a usual expression (Buchmann 1996; Kunz et al. 2002).

$$N_A \langle \sigma v \rangle^{AF} = \frac{a_0}{T_9^2 (1 + a_1 T_9^{-2/3})^2} \exp\left[-\frac{a_2}{T_9^{1/3}} - \left(\frac{T_9}{a_3} \right)^2 \right] + \frac{a_4}{T_9^2 (1 + a_5 T_9^{-2/3})^2} \exp\left(-\frac{a_6}{T_9^{1/3}} \right) + \frac{a_7}{T_9^{3/2}} \times \exp\left(-\frac{a_8}{T_9} \right) + \frac{a_9}{T_9^{2/3}} (1 + a_{10} T_9^{1/3}) \exp\left(-\frac{a_{11}}{T_9^{1/3}} \right). \quad (2)$$

The difference between the fitting formula to the tabulated rate is shown in Figure 3(F). The blue bands indicate the uncertainty of the adopted rate in Table 1. The dotted line shows the ratio of the adopted values of the analytical expression normalized to the adopted tabulated ones. It is applicable in the temperature range of $0.04 \leqslant T_9 \leqslant 10$ with a maximum deviation of 4% to the recommended rate in Table 1. For the most important range of $T_9 = 0.1$–0.3 the maximal deviation is 1%. And the parameters $a_0 - a_{11}$ are $a_0 = 4.70 \times 10^8$; $a_1 = 0.312$; $a_2 = 31.8$; $a_3 = 400$; $a_4 = 1.08 \times 10^{15}$; $a_5 = 23.6$; $a_6 = 41.3$; $a_7 = 2.49 \times 10^3$; $a_8 = 28.5$; $a_9 = 1.19 \times 10^{11}$; $a_{10} = -98.0$; $a_{11} = 36.5$.

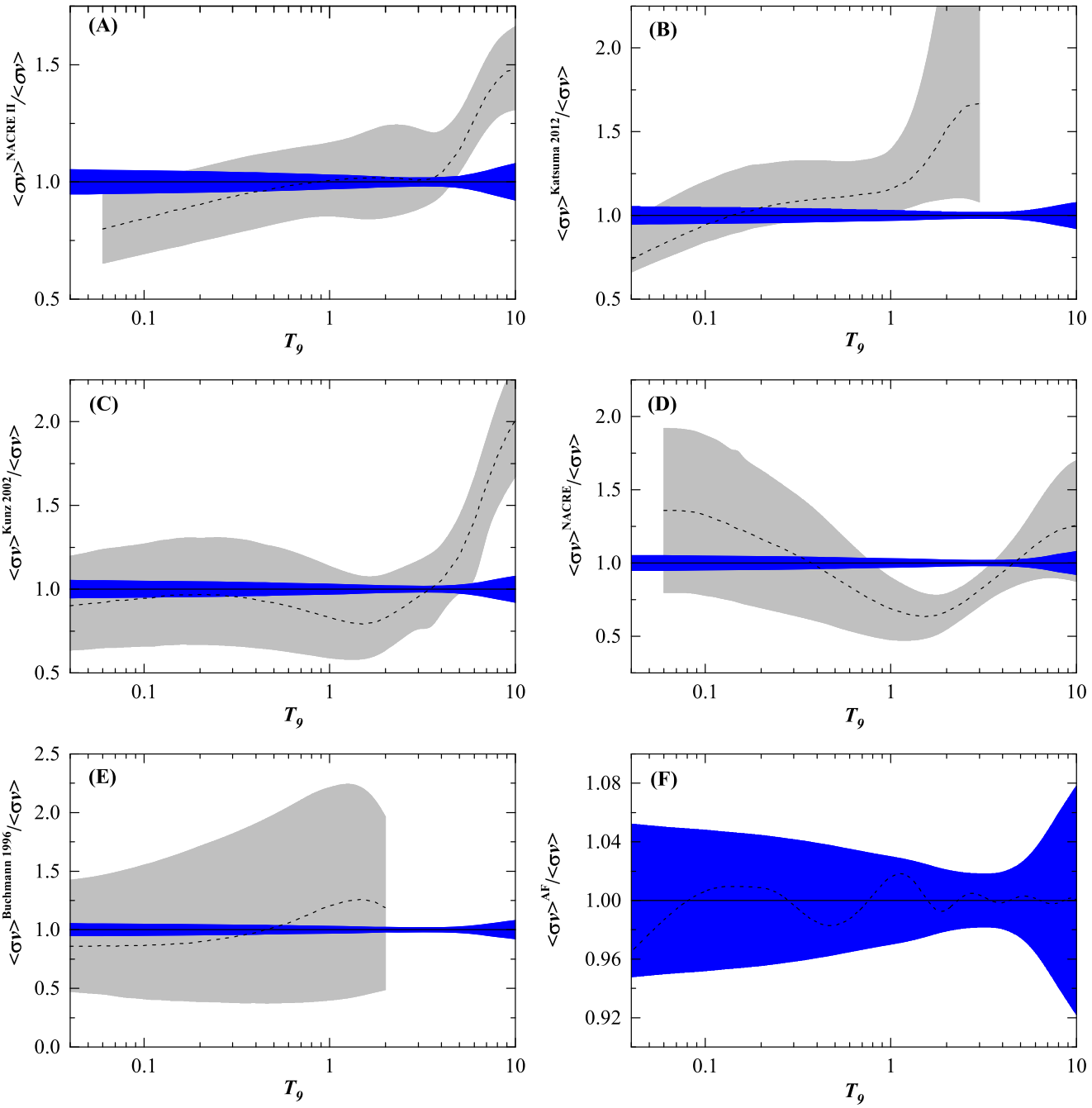

Figure 3. Comparisons (ratio) of $^{12}C(\alpha, \gamma)^{16}O$ reaction rates from the compilations of (A) NACRE II, (B) Katsuma (2012), (C) Kunz et al. (2002), (D) NACRE, and (E) Buchmann (1996) with our new recommended rate. The accuracy of the analytic formula according to Equation (2) is shown in Figure 3(F).

3. CONCLUSIONS

New $^{12}C(\alpha, \gamma)^{16}O$ reaction rates in the range of $0.04 \leqslant T_9 \leqslant 10$ have been estimated from recent S factor modeling. The measurements at higher energies are analyzed in our R-matrix fit, which significantly reduce the uncertainty of the reaction rate at higher temperatures. A comprehensive comparison is done between our results and the previous data. It should be noted that the results are obtained by the theoretical extrapolation of existing experimental data from the ^{16}O system. There could be some important factors that our model does not include. Additional experiments and theoretical work are needed to further validate existing expressions for the $^{12}C(\alpha, \gamma)^{16}O$ rate.

From Figures 1 and 2, it is suggested that an improved investigation of $S_{\rm casc}$ and $S_{\rm tot}$ at 1_3^- and 1_4^- resonances, may help to further reduce the uncertainties of reaction rates at higher temperatures. Moreover, the ANCs of the corresponding states are not consistent with each other in the transfer reaction (Brune et al. 1999; Belhout et al. 2007; Oulebsir et al. 2012; Avila et al. 2015), causing a large amount of uncertainty, which remains to be solved. Finally, the extrapolated $S_{\rm tot}(0.3\,{\rm MeV})$ is quite sensitive to the data that are as close as possible to the Gamow window. The reverse reaction (γ, α) using a high photon flux γ-ray beam, such as the High Intensity γ-ray Source at TUNL (Gai 2012; DiGiovine et al. 2015) and Shanghai Laser Electron Gamma Source facility (Xu

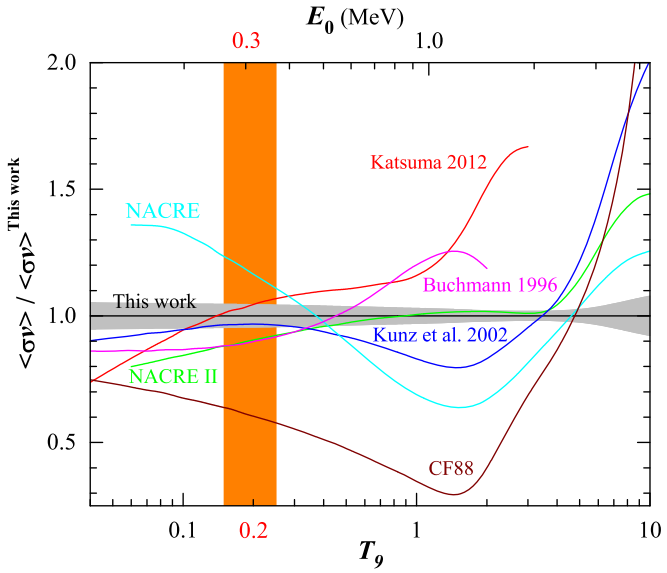

Figure 4. Comparisons of the astrophysical reaction rate of $^{12}C(\alpha, \gamma)^{16}O$ (including CF88) normalized to our new recommended rate.

et al. 2007; Luo et al. 2011), which is still under construction, would be desirable in order to allow for the measurement of cross sections in the pb region.

The authors would like to thank Prof. Stan Woosley and Prof. Alexander Heger for helpful discussions of reaction rates. This work is partially supported by the National Natural Science Foundation of China under Grant Nos. 11175233, 91126017, and 11421505 and the 973 project under contract no. 2014CB845401.

REFERENCES

An, Z. D., Chen, Z. P., Ma, Y. G., et al. 2015, PhRvC, 92, 045802
Angulo, C., Arnould, M., Rayet, M., et al. 1999, NuPhA, 656, 3 (NECRE)
Avila, M. L., Rogachev, G. V., Koshchiy, E., et al. 2015, PhRvL, 114, 071101
Azuma, R. E., Uberseder, E., Simpson, E. C., et al. 2010, PhRvC, 81, 045805
Belhout, A., Ouichaoui, S., Beaumevieille, H., et al. 2007, NuPhA, 793, 178
Brochard, F., Chevallier, P., Disdier, D., et al. 1973, J. Phys. France, 34, 363
Brown, E. F., & Bildsten, L. 1998, ApJ, 496, 915
Brown, G. E., Heger, A., Langer, N., et al. 2001, NewA, 6, 457
Brune, C. R., Geist, W. H., Kavanagh, R. W., et al. 1999, PhRvL, 83, 4025
Buchmann, L. 1996, ApJL, 468, L127
Caughlan, G. R., & Fowler, W. A. 1988, ADNDT, 40, 283 (CF88)
deBoer, R. J., Görres, J., Imbriani, G., et al. 2013, PhRvC, 87, 015802
DiGiovine, B., Henderson, D., Holt, R. J., et al. 2015, NIMPA, 781, 96
Dominguez, I., Höflich, P., & Straniero, O. 2001, ApJ, 557, 279
Fowler, W. A. 1984, RvMP, 56, 149
Fynbo, H. O. U., Diget, C. A., Bergmann, U. C., et al. 2005, Natur, 433, 136
Gai, M. 2012, JPhCS, 337, 012054
Katsuma, M. 2008, PhRvC, 78, 034606
Katsuma, M. 2012, ApJ, 745, 192
Kunz, R., Jaeger, M., Mayer, A., et al. 2002, ApJ, 567, 643
Luo, W., Xu, W., Pan, Q. Y., et al. 2011, NIMPA, 660, 108
Ma, C. W., Lv, C. J., Wei, H. L., et al. 2014, NST, 25, 040501
Ophel, T. R., Frawley, A. D., Treacy, P. B., & Bray, K. H. 1976, NuPhA, 273, 397
Oulebsir, N., Hammache, F., Roussel, P., et al. 2012, PhRvC, 85, 035804
Rolfs, C. E., & Rodney, W. S. 1988, Cauldrons in the Cosmos (Chicago, IL: Univ. Chicago Press)
Schürmann, D., Di Leva, A., De Cesare, N., et al. 2005, EPJA, 26, 301
Schürmann, D., Di Leva, A., Gialanella, L., et al. 2011, PhLB, 703, 557
Schürmann, D., Gialanella, L., Kunz, R., & Strieder, F. 2012, PhLB, 711, 35
Smith, D. L. 1991, Probability, Statistics, and Data Uncertainties in Nuclear Science and Technology (Amer Nuclear Society: Chicago)
Tilley, D. R., Weller, H. R., & Cheves, C. M. 1993, NuPhA, 564, 1
Tur, C., Heger, A., & Austin, S. 2010, ApJ, 718, 357
Wen, D. H., & Zhou, Y. 2013, NST, 24, 050508
Woosley, S. E., & Heger, A. 2007, PhR, 442, 269
Woosley, S. E., Heger, A., Weaver, T. A., et al. 2003, NuPhA, 718, 3c
Xu, Y., Takahashi, K., Goriely, S., et al. 2013, NuPhA, 918, 61 (NACREII)
Xu, Y., Xu, W., Ma, Y. G., et al. 2007, NIMPA, 581, 866